Superconductivity in the doped Hubbard model and its interplay with next-nearest hopping t'

Hong-Chen Jiang[1]* and Thomas P. Devereaux[1,2]

The Hubbard model is widely believed to contain the essential ingredients of high-temperature superconductivity. However, proving definitively that the model supports superconductivity is challenging. Here, we report a large-scale density matrix renormalization group study of the lightly doped Hubbard model on four-leg cylinders at hole doping concentration δ = 12.5%. We reveal a delicate interplay between superconductivity and charge density wave and spin density wave orders tunable via next-nearest neighbor hopping t'. For finite t', the ground state is consistent with a Luther-Emery liquid with power-law superconducting and charge density wave correlations associated with half-filled charge stripes. In contrast, for $t' = 0$, superconducting correlations fall off exponentially, whereas charge density and spin density modulations are dominant. Our results indicate that a route to robust long-range superconductivity involves destabilizing insulating charge stripes in the doped Hubbard model.

In the two-dimensional Hubbard model, the close competition between a number of near-degenerate ground states makes it difficult to determine whether the model supports the presence of robust superconducting (SC) order (1). Finite temperature studies using cluster dynamical mean field theory indicate a transition into a uniform d-wave SC state at temperatures ~0.02t (where t is the hopping integral) (2). However, extensive studies using the density matrix renormalization group (DMRG), particularly around δ = 12.5% hole doping concentration, indicate that the charge density wave (CDW) and spin density wave (SDW) orders in the form of "stripes" provide dominant correlations, with SC correlations being subleading and decaying exponentially with lattice size (3–5). In addition, the filling of the stripes and their wavelength depends strongly on next-nearest neighbor hopping t', with a much smaller dependence on Hubbard Coulomb repulsion U, reflecting a flat energy landscape for different stripe configurations in Hubbard ladders (3, 5, 6). This raises the possibility that the delicate interplay between stripe and SC orders causes the underlying SC state of the Hubbard model to be particularly sensitive to t', as discussed empirically and in the context of the role of axial orbitals (7).

Here, we report extensive DMRG studies of the $t - t' - U$ Hubbard model at hole doping concentration δ = 12.5% on four-leg cylinders with periodic and open boundary conditions in short and long directions, respectively. By explicitly keeping a large number of states, we demonstrate that the equal-time SC and CDW correlations are long ranged. Consistent with Luther-Emery (LE)

liquid (8), this demonstrates a close interplay between charge and SC correlations. Moreover, we show that the results depend strongly on t', which tips the balance between charge density and SC correlations. Specifically, we find "filled" insulating charge stripes of wavelength λ = 1/δ and a lack of long-range superconductivity for $t' = 0$, which is consistent with prior results (3, 5). For finite $t' < 0$, the insulating charge stripes are replaced with weaker "half-filled" stripes with a shorter period λ = 1/δ, and, concomitantly, the SC correlations become long ranged. A LE liquid was also predicted to exist in the lightly doped two-leg ladders (9–13) and was confirmed by a recent DMRG study (14). Here, we show that the LE liquid also exists in Hubbard systems with long-range SC correlations on cylinders or ladders that have widths in excess of two legs, with a delicate interplay with doping of charge stripes and superconductivity turned by t'.

Solving the Hubbard model with DMRG

We employ the DMRG (15) to investigate the ground-state properties of the hole-doped Hubbard model on the square lattice defined by the Hamiltonian

$$H = -\sum_{ij\sigma} t_{ij}(\hat{c}^+_{i\sigma}\hat{c}_{j\sigma} + h.c.) + U\sum_i \hat{n}_{i\uparrow}\hat{n}_{i\downarrow} \quad (1)$$

where $\hat{c}^+_{i\sigma}$ ($\hat{c}_{i\sigma}$) is the electron creation (annihilation) operator on site $i = (x_i, y_i)$ with spin σ, $\hat{n}_i = \sum_\sigma \hat{c}^+_{i\sigma}\hat{c}_{i\sigma}$ is the electron number operator, and h.c. is the Hermitian conjugate. The electron-hopping amplitude t_{ij} is equal to t if i and j are nearest neighbors and equal to t' for next-nearest neighbors. U is the on-site repulsive Coulomb interaction. We take the lattice geometry to be cylindrical and a lattice spacing of unity. The boundary condition of the cylinders is periodic in

the $\hat{y} = (0, 1)$ direction and open in the $\hat{x} = (1, 0)$ direction. Here, we focus on cylinders with width L_y and length L_x, where L_y and L_x are number of sites along the $\hat{y}$ and $\hat{x}$ directions, respectively. There are $N = L_x \times L_y$ lattice sites, and the number of electrons is $N_e = N$ at half-filling; i.e., $\hat{n}_i = 1$. The concentration of doped holes is defined as δ = $\frac{N_h}{N}$ with $N_h = N - N_e$ the number of holes, which is $N_h = 0$ at half-filling.

For the present study, we focus on the lightly doped case at hole concentration δ = 12.5% on cylinders with width $L_y = 4$ and length up to $L_x = 64$. We set $t = 1$ as an energy unit and report results for $t' = -0.25$ with interactions $U = 8$ and 12. For comparison, the case with $t' = 0$ is also considered. In our calculations, the total magnetization is fixed at zero, and we perform ~60 sweeps and keep up to $m = 20{,}000$ states in each DMRG block with a typical truncation error ε ~ 1 × 10⁻⁶ for $t' = -0.25$ and ε ~ 3 × 10⁻⁶ for $t' = 0$. This leads to excellent convergence for our results when extrapolated to the $m = \infty$ limit. Further details of the numerical simulation are provided in (16).

Principal results

We have investigated the ground-state properties of the Hubbard model on a $L_y = 4$ cylinder at doping level concentration δ = 12.5% with interaction $U = 8$ and 12. For $t' = 0$, we find that the system forms charge stripes of wavelength λ = 1/δ (i.e., λ = 8) (Fig. 1A) and antiferromagnetic ordering with a modulation of wavelength λ = 2/δ (i.e., λ = 1/6). Consistent with Hartree-Fock calculations (17–19) and previous numerical studies (3, 5), these charge stripes carry a wave vector $Q = 2\pi\delta$ and so there is one doped hole per unit cell (Fig. 1A); this state is referred to as "filled" stripes. However, we find that these filled stripes are not stable with respect to small finite values, where $t' = -0.25$ is sufficient to drive the system into a different type of charge stripe (Fig. 1B). In contrast to filled stripes, the new stripes carry an ordering vector $Q = 4\pi\delta$ of wavelength λ = 1/δ (i.e., λ = 4), with only half a doped hole per unit cell (Fig. 1B); this state is referred to as "half-filled" stripes.

Because $L_x \gg L_y$, our system can be thought of as one-dimensional, and we find that the ground state is always in a LE phase (8) characterized by gapless charge excitation (Figs. 2 and 3) and a gap in the spin sector (Fig. 4), with one gapless charge mode (Fig. 5). At long distances, the spatial decay of the charge density correlation $A_{cdw}(L_x)$ and the SC pair-field correlation $\Phi(r)$ (defined in Eq. 3) is dominated by a power law (Fig. 3) with the corresponding Luttinger exponents K_c and K_{sc} defined by

$$A_{cdw}(L_x) \propto L_x^{-K_c/2} \text{ and } \Phi(x) \propto |x|^{-K_{sc}} \quad (2)$$

where x is the displacement along the cylinder $1 \ll |x| \ll L_x$. As expected theoretically from the LE liquid (8), we find that the relation $K_cK_{sc} = 1$ holds within the numerical uncertainty (Table 1). This is in sharp contrast to findings of previous studies (3, 5) without a next-nearest neighbor electron-hopping term (i.e., $t' = 0$), where the filled stripes

[1]Stanford Institute for Materials and Energy Sciences, SLAC and Stanford University, Menlo Park, CA 94025, USA. [2]Geballe Laboratory for Advanced Materials, Stanford University, Stanford, CA 94305, USA.
*Corresponding author. Email: hcjiang@stanford.edu
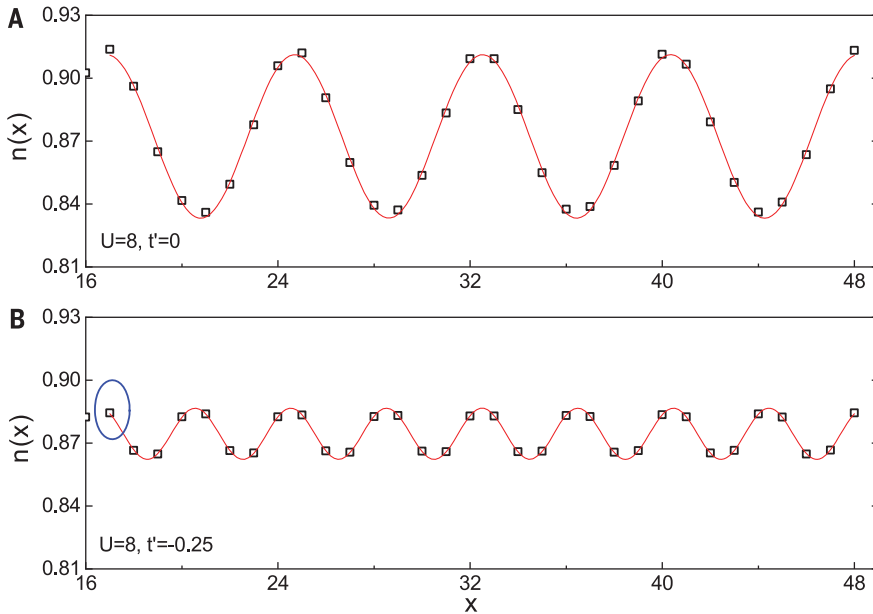
Fig. 1. Charge density profiles. Shown are the CDW profiles $n(x)$ for the Hubbard model at doping level $\delta = 12.5\%$ on $L_x = 64$ cylinders at $U = 8$ with $m = 20,000$ for (**A**) $t' = 0$ and (**B**) $t' = -0.25$. Black squares denote numerical data; red lines are fitting curves to the function $n(x) = A_{cdw}\cos(Qx + \theta) + n_0$, where A_{cdw} and Q are the CDW amplitude and ordering wave vector, respectively, and θ is the phase shift. Note that only the central-half region with rung indices $x = \frac{L_x}{4} + 1$ to $\frac{3L_x}{4}$ is shown and used in the fitting, whereas the remaining $\frac{L_x}{4}$ data points from each end are removed to minimize boundary effects. The blue oval denotes the reference site (see text).

persist in the limit $L_x = \infty$ while a quasi–long-range SC correlation is absent. Our finding is, however, consistent with recent DMRG results from the lightly doped t-J model (in which J is the coupling constant) on four-leg cylinders with half-filled charge stripes (*20*).

As the interaction is decreased from $U = 12$ to 8, the CDW correlations become weaker (Fig. 2B), whereas the SC correlations become stronger (Fig. 3B). These numerical observations indicate that the CDW and SC orders may be mutually competing, consistent with recent experiments on cuprates. Moreover, calculations show that spin-spin correlations are the dominant correlations at short distances; however, they decay exponentially at longer distances, allowing SC correlations to be dominant at long distances (Fig. 4). This short-range antiferromagnetic order with gapped spin excitations for $t' < 0$ is contrary to the case of $t' = 0$, where the spin-spin correlations may be long ranged (*3*, *21*), preventing the growth of SC correlations. Therefore, t' clearly is a control parameter that tips a delicate balance between CDW, SDW, and SC correlations.

Charge density wave order

To describe the charge density properties of the ground state, we define the local rung density operator as $\hat{n}(x) = \frac{1}{L_y}\sum_{y=1}^{L_y}\hat{n}(x, y)$ and its expectation value as $n(x) = \langle\hat{n}(x)\rangle$. Figure 1A shows the charge density distribution $n(x)$ in a central portion of a cylinder with $L_x = 64$ at $U = 8$ and $t' = 0$, in which the filled charge stripe of wavelength $\lambda = 8$ is found, consistent with previous studies (*3–5*, *17*). The spin-spin correlations are antiferromagnetic with a π-phase shift every eight sites, as expected. A quasi–long-range SC correlation in this case is unlikely because the charge stripes are completely filled with holes and are therefore insulating (*5*, *16*). Nota-
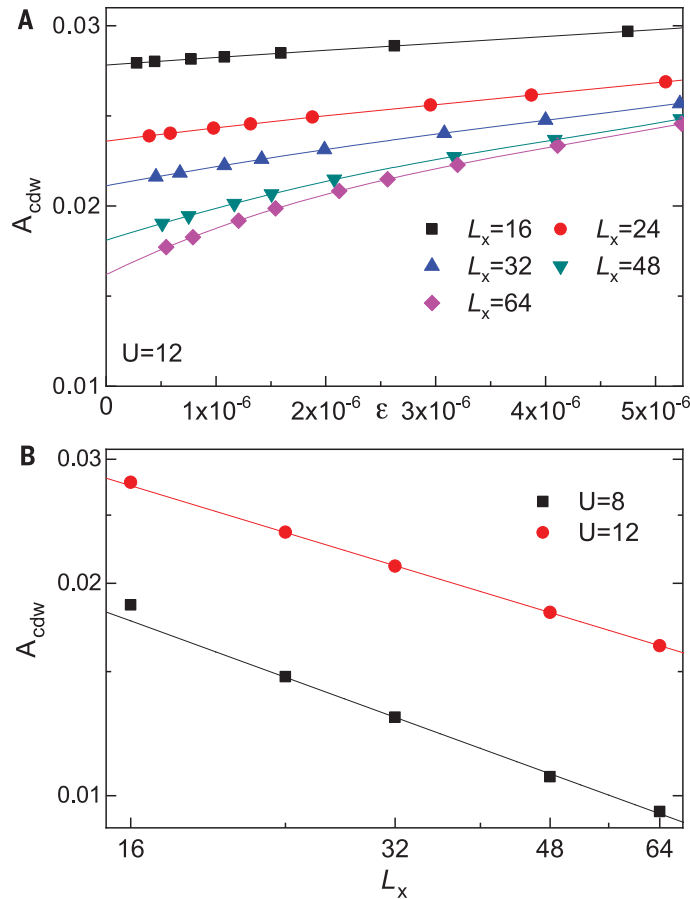
Fig. 2. CDW amplitude A_{cdw}. (**A**) Convergence and length dependence of the CDW amplitude $A_{cdw}(L_x)$ for $\delta = 12.5\%$ at $t' = -0.25$ and $U = 12$ with L_x ranging between 16 and 64. Solid lines denote fittings using quartic polynomials. The x axis shows the truncation error ε. (**B**) Finite-size scaling: $A_{cdw}(L_x)$ as a function of L_x in a double-logarithmic plot for both $U = 8$ and 12.

bly, we find that a finite $t' = -0.25t$ is sufficient to destroy the insulating charge stripes, and the half-filled stripes of wavelength $\lambda = 4$ appear accordingly (Fig. 1B). A key difference between Fig. 1A and Fig. 1B is that this half-filled charge stripe is much weaker than the filled charge

stripe [its modulation amplitude $A_{cdw}(L_x)$ is considerably weaker].

For a given L_x cylinder, the CDW amplitude $A_{cdw}(L_x)$ can be obtained by extrapolating to the limit $m = \infty$ or $\varepsilon = 0$ from the values extracted from fits to the data, such as in Fig. 1.

Figure 2A plots the CDW amplitude A_{cdw} for cylinders of length L_x ranging from 16 to 64 at $U = 12$ by keeping $m = 4096$ to 20,000 states with corresponding truncation error ε determined by DMRG calculation (15). In DMRG simulation, accurately describing the behavior of physical observables such as $A_{cdw}(L_x)$ and correlation functions such as $\Phi(x)$ at longer distances requires an increasing number of states; higher-order terms in the extrapolation become more important. Therefore, in addition to retaining a very large number of states, we perform a quartic polynomial fitting to capture the effect of possible higher-order terms in the extrapolation. For all cases, we find that this procedure works very well with the linear regression R^2 always larger than 99.99%. Further details concerning the reliability of this extrapolation are presented in (16).

The results from finite-size scaling of the obtained $A_{cdw}(L_x)$ as a function of L_x are given in Fig. 2B for $t' = -0.25$ at both $U = 8$ and 12. In the double-logarithmic plot, our results for both

$U = 8$ and 12 are approximately linear, indicating that $A_{cdw}(L_x)$ decays with a power law and vanishes in the limit $L_x = \infty$. The exponent K_c, which is shown in Table 1, was obtained by fitting the data points using Eq. 2. K_c can also be obtained directly from the Friedel oscillations of the charge density modulation near the end of the cylinders, producing similar results. Further details can be found in (16).

Superconducting correlation

To test the possibility of superconductivity, we have calculated the equal-time pair-field correlation functions. Because the ground state of the system with an even number of doped holes is always found to have zero spin, we focus on spin-singlet pairing. A diagnostic of the SC order is the pair-field correlator, defined as

$$\Phi_{\alpha\beta}(x) = \frac{1}{L_y}\sum_{y=1}^{L_y}\langle \Delta_\alpha^\dagger(x_0, y)\Delta_\beta(x_0 + x, y)\rangle \quad (3)$$

Here, $\Delta_\alpha^\dagger(x, y)$ is the spin-singlet pair-field creation operator given by $\Delta_\alpha^\dagger(x, y) = \frac{1}{\sqrt{2}}\left[c_{(x,y),\uparrow}^\dagger c_{(x,y)+\alpha,\downarrow}^\dagger - c_{(x,y),\downarrow}^\dagger c_{(x,y)+\alpha,\uparrow}^\dagger\right]$, where the bond orientations are designated $\alpha = \hat{x}, \hat{y}$; (x_0, y) is the reference bond indicated by the blue oval as shown in Fig. 1; and x is the distance between two bonds in the $(1, 0)$ direction.

Owing to the presence of CDW modulations (Fig. 1), SC correlations $\Phi_{\alpha\beta}(x)$ exhibit spatial oscillations similar to those of $n(x)$. This modulation, together with a pronounced boundary effect due to open ends of the cylinder, makes it very difficult to accurately determine the decay of SC correlations. This could be one of the main reasons that previous studies have had difficulty in providing direct evidence for (quasi)–long-ranged superconductivity (3, 21).

We determine the decay of SC correlations by simultaneously minimizing the effects induced by both CDW modulations and open boundary conditions. Instead of directly fitting $\Phi_{\alpha\beta}(x)$, we calculate the SC correlation $\Phi_{\alpha\beta}(L_x/2)$ for a given cylinder of length L_x, with the reference bond located at the peak position around $x_0 \sim L_x/4$ of the charge density distribution. Examples of $\Phi_{yy}(L_x/2)$ are shown in Fig. 3A for cylinders of length L_x ranging from 16 to 64. Notably, we find that the SC correlations are much stronger for bonds along the width of cylinder Φ_{yy} than along the length Φ_{xx}, indicating a possible equal superposition of d-wave and extended s-wave pairing stemming from the explicit breaking of C_4 symmetry on the cylinder.

For each cylinder of length L_x, we extrapolate $\Phi_{yy}(L_x/2)$ to the limit $\varepsilon = 0$ using a quartic polynomial fit with a linear regression R^2 larger than 99.97%. This gives accurate values of $\Phi_{yy}(L_x/2)$ for reliable finite scaling. More details of the extrapolation are presented in (16). Figure 3 shows examples of the finite-size scaling of Φ_{yy} for both $U = 8$ and 12. Similar to $A_{cdw}(L_x)$, it decays with a power law, whose exponent K_{sc}, given in Table 1, was obtained by fitting the results using Eq. 2. Therefore, we can conclude that the ground state of the lightly doped Hubbard model at doping level $\delta = 12.5\%$ on width $L_y = 4$ cylinders with $t' = -0.25$ has quasi–long-range SC correlations. This finding is in stark contrast to the case for $t' = 0$, where SC correlations decay exponentially and the stripes are filled (Fig. 1A and fig. S5B).
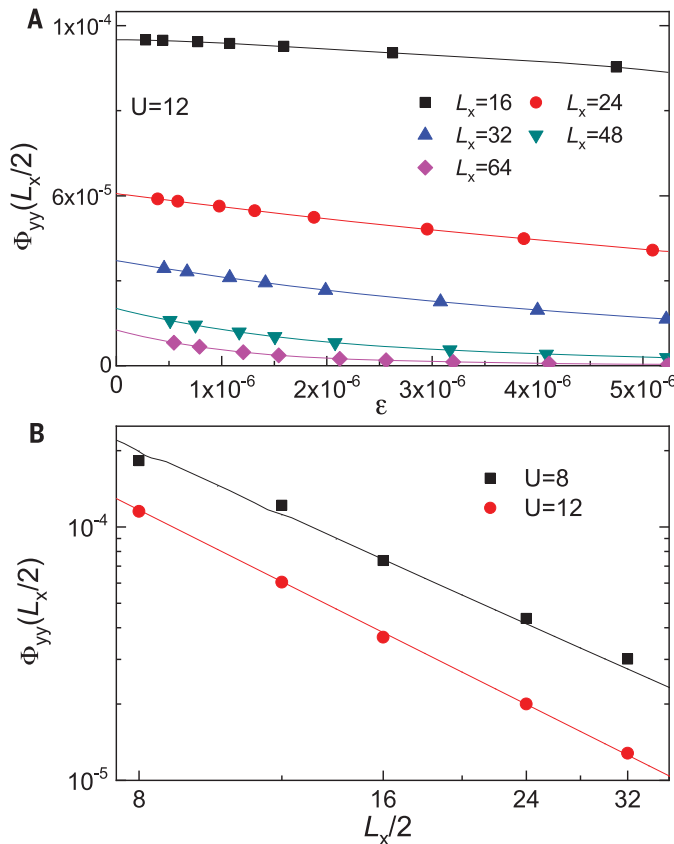
Spin-spin correlation

To describe the magnetic properties of the ground state, we have also calculated the spin-spin correlation functions defined as

$$F(x) = \frac{1}{L_y}\sum_{y=1}^{L_y}\left|\left\langle \vec{S}_{x_0,y} \cdot \vec{S}_{x_0+x,y}\right\rangle\right| \quad (4)$$

where $\vec{S}_{x,y}$ is the spin operator on site $i = (x, y)$. (x_0, y) is the reference site indicated by the blue oval shown in Fig. 1, and x is the distance between two sites in the $\hat{x}$ direction. Following the same procedure as for $A_{cdw}(L_x)$ and $\Phi_{yy}(L_x/2)$,

Fig. 3. SC correlation function. (**A**) SC correlation function $\Phi_{yy}(L_x/2)$ for $\delta = 12.5\%$ at $t' = -0.25$ and $U = 12$ with L_x ranging from 16 to 64. Solid lines denote quartic polynomial fits. (**B**) Finite-size scaling of $\Phi_{yy}(L_x/2)$ as a function of L_x in a double-logarithmic plot for both $U = 8$ and 12.


Table 1. Luttinger exponents. The table lists the exponents K_c and K_{sc}, as well as spin-spin correlation length ξ_s of the Hubbard model at doping level $\delta = 12.5\%$ and $t' = -0.25$. Here, $t = 1$.

U	K_c	K_{sc}	$K_c K_{sc}$	ξ_s
8	0.94(4)	1.35(5)	1.25(8)	10.3(4)
12	0.74(4)	1.59(7)	1.18(12)	8.4(4)
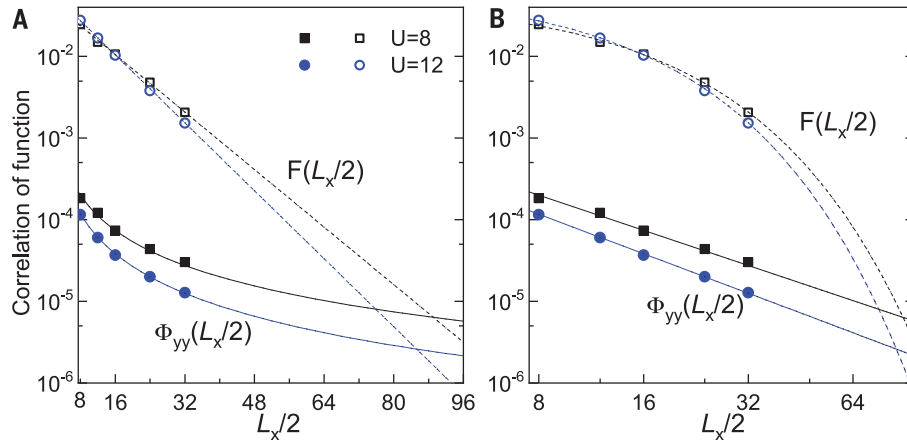
Fig. 4. Comparison between SC and spin-spin correlations. SC $\Phi_{yy}(L_x/2)$ and spin-spin $F(L_x/2)$ correlations at doping level $\delta = 12.5\%$ at $t' = -0.25$ for $U = 8$ and 12 on (**A**) semi-logarithmic and (**B**) double-logarithmic scales, as a function of L_x. Solid lines denote the power-law fitting $\Phi_{yy}(L_x/2) \propto (L_x/2)^{-K_{sc}}$, whereas dashed lines denote the exponential fitting $F(r) \propto e^{-L_x/2\xi_s}$, where ξ_s is the spin-spin correlation length given in Table 1.

Fig. 5. Von Neumann entanglement entropy, S. S is shown at doping level $\delta = 12.5\%$ and $t' = -0.25$ for $U = 8$ and 12 as a function of the cylinder length L_x. (Inset) Extracted central charge c as a function of U. The dashed line marks $c = 1$. Here, $t = 1$. Error bars denote the uncertainty caused by finite size effect.
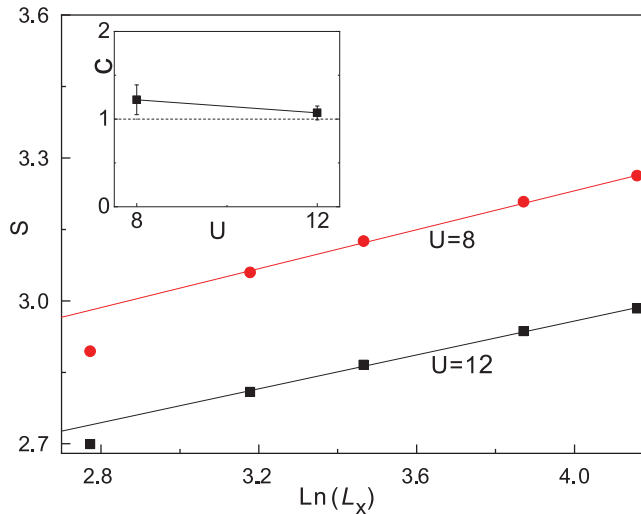
we first extrapolate $F(L_x/2)$ for a given cylinder of length L_x to the limit $m = \infty$ and then perform finite-size scaling as a function of L_x. As shown in Fig. 4B, $F(L_x/2)$ decays exponentially with L_x—i.e., $F(L_x/2) \propto e^{-L_x/2\xi_s}$—with a corresponding spin-spin correlation length ξ_s of 8 to 10 lattice spacings (Table 1). Therefore, we conclude that the spin-spin correlations are short ranged with a finite gap in the spin sector. Again, this is in sharp contrast to the case of $t' = 0$, reflecting the metallic nature of the doped stripes.

Although the spin-spin correlations decay exponentially with L_x, they are still dominant over SC correlations up to relatively long distances. To observe this behavior, we make a direct comparison between the spin-spin and SC correlations in the same plot in Fig. 4 using both double-logarithmic and semi-logarithmic scales. The comparison suggests that relatively large systems, such as $L_x \sim 180$ cylinders, are nec-

essary to observe dominant long-range SC correlations. This point stresses the importance of cylinder length and convergence in DMRG studies (*16*).

Central charge

A key feature of the LE liquid is that it has a single gapless charge mode with central charge $c = 1$, which can be obtained by calculating the von Neumann entropy $S = -\text{tr}(\rho\ln\rho)$, where ρ is the reduced density matrix of a subsystem with length l. For critical systems in $1 + 1$ dimensions described by a conformal field theory (CFT), it has been established (*22*) that $S(l) = \frac{c}{6}\ln(l) + \tilde{c}$ for open systems, where c is the central charge of the CFT and $\tilde{c}$ denotes a model-dependent constant. For finite cylinders with length L_x, we can fix $l = \frac{L_x}{2}$ to extract c. Figure 5 shows $S(\frac{L_x}{2})$ for both $U = 8$ and 12. The inset shows the fitted c as a function of U. Although the ex-

tracted value of c is slightly larger than 1, we suspect that this is due to the truncation error ε extrapolation and finite-size effect. The result is consistent with one gapless charge mode with $c = 1$, which thus provides additional evidence for the presence of a LE liquid in the doped Hubbard model.

Discussion

Taken together, our DMRG results indicate that the filling of stripes is a key ingredient that controls the balance between CDW and SDW order and superconductivity, with the next-nearest neighbor hopping t' being a key tuning parameter to destabilize filled insulating charge stripes. Our results indicate that a route toward stable long-range SC order may lie in mechanisms that perturb the balance between various intertwined correlations. Most likely, t' alone is not solely responsible for depopulating filled charge stripes in real materials, as other factors such as longer-range hoppings, other orbital contributions, and dynamical lattice effects may also destabilize insulating charge stripes. Answering these open questions may lead to a better understanding of the robust superconductivity observed in cuprates.

REFERENCES AND NOTES

1. P. Corboz, T. M. Rice, M. Troyer, *Phys. Rev. Lett.* **113**, 046402 (2014).
2. P. Staar, M. Jiang, U. R. Hähner, T. C. Schulthess, T. A. Maier, *Phys. Rev. B* **93**, 165144 (2016).
3. B.-X. Zheng *et al.*, *Science* **358**, 1155–1160 (2017).
4. E. W. Huang *et al.*, *Science* **358**, 1161–1164 (2017).
5. G. Ehlers, S. R. White, R. M. Noack, *Phys. Rev. B* **95**, 125125 (2017).
6. E. W. Huang, C. B. Mendl, H. C. Jiang, B. Moritz, T. P. Devereaux, *npj Quantum Mater.* **3**, 22 (2018).
7. E. Pavarini, I. Dasgupta, T. Saha-Dasgupta, O. Jepsen, O. K. Andersen, *Phys. Rev. Lett.* **87**, 047003 (2001).
8. A. Luther, V. J. Emery, *Phys. Rev. Lett.* **33**, 589–592 (1974).
9. E. Dagotto, J. Riera, D. Scalapino, *Phys. Rev. B* **45**, 5744–5747 (1992).
10. H. Tsunetsugu, M. Troyer, T. M. Rice, *Phys. Rev. B* **49**, 16078–16081 (1994).
11. M. Troyer, H. Tsunetsugu, T. M. Rice, *Phys. Rev. B* **53**, 251–267 (1996).
12. E. Dagotto, T. M. Rice, *Science* **271**, 618–623 (1996).
13. L. Balents, M. P. A. Fisher, *Phys. Rev. B* **53**, 12133–12141 (1996).
14. M. Dolfi, B. Bauer, S. Keller, M. Troyer, *Phys. Rev. B* **92**, 195139 (2015).
15. S. R. White, *Phys. Rev. Lett.* **69**, 2863–2866 (1992).
16. See supplementary materials.
17. J. Zaanen, O. Gunnarsson, *Phys. Rev. B* **40**, 7391–7394 (1989).
18. K. Machida, *Physica C* **158**, 192–196 (1989).
19. H. J. Schulz, *Phys. Rev. Lett.* **64**, 1445–1448 (1990).
20. H. C. Jiang, Z. Y. Weng, S. A. Kivelson, *Phys. Rev. B* **98**, 140505 (2018).
21. J. F. Dodaro, H.-C. Jiang, S. A. Kivelson, *Phys. Rev. B* **95**, 155116 (2017).
22. P. Calabrese, J. Cardy, *J. Stat. Mech.* **2004**, P06002 (2004).
23. H.-C. Jiang, Data for "Superconductivity in the doped Hubbard model and its interplay with next-nearest hopping t'," version v2, Zenodo (2019); https://doi.org/10.5281/zenodo.3368664.
24. H.-C. Jiang, Source code for "Superconductivity in the doped Hubbard model and its interplay with next-nearest hopping t'," version 1, Zenodo (2019); https://doi.org/10.5281/zenodo.2651698.

Science

Superconductivity in the doped Hubbard model and its interplay with next-nearest hopping t'

Hong-Chen Jiang and Thomas P. Devereaux

Tweaking the Hubbard model

Modeling high-temperature superconductivity (HTS) remains extremely challenging. Many researchers believe that the simplest model that captures HTS is the Hubbard model, which accounts for interactions and allows for electrons to hop from one site of a lattice to another. However, even just determining whether the ground state of this model supports superconductivity is tricky. Jiang and Devereaux undertook an extensive computational study based on a method known as density matrix renormalization group. They found that for a particular concentration of empty lattice sites, superconductivity indeed appears as a long-range state, but only if electrons are allowed to hop to sites that are next to their immediate neighbors on the lattice.

Science, this issue p. 1424

ARTICLE TOOLS	http://science.sciencemag.org/content/365/6460/1424
SUPPLEMENTARY MATERIALS	http://science.sciencemag.org/content/suppl/2019/09/25/365.6460.1424.DC1
REFERENCES	This article cites 24 articles, 3 of which you can access for free http://science.sciencemag.org/content/365/6460/1424#BIBL
PERMISSIONS	http://www.sciencemag.org/help/reprints-and-permissions